vol. 46/2, edited by K. Sitte, pp. 551–612, Springer, New York, 1967.
Lal, D., and V. S. Venkatavaradan, Activation of cosmic dust by cosmic-ray particles, *Earth Planet. Sci. Lett., 3,* 299–310, 1967.
Lal, D., R. S. Rajan, and V. S. Venkatavaradan, Nuclear effects of 'solar' and 'galactic' cosmic-ray particles in near-surface regions of meteorites, *Geochim. Cosmochim. Acta, 31,* 1859–1869, 1967.
Lal, D., D. Macdougall, L. Wilkenig, and G. Arrhenius, Mixing of the lunar regolith and cosmic ray spectra; Evidence from particle track studies, *Geochim. Cosmochim. Acta,* suppl. 1, vol. 3, 2295–2303, 1970.
Lavrukhina, A. K., and G. K. Ustinova, Solar proton medium flux constancy over a million years, *Nature, 232,* 462–463, 1971.
Malitson, H. H., and W. R. Webber, Summary of solar cosmic-ray events, Solar Proton Manual, *NASA Tech. Rep. R-169,* 1963.
Mason, B., *Meteorites,* pp. 154–164, John Wiley, New York, 1962.
McGowan, F. K., W. T. Milner, and H. J. Kim, Nuclear cross sections for charged particle induced reactions; Mn, Fe, Co, *Rep. CPX-1,* pp. 140–141, Oak Ridge National Lab., Oak Ridge, Tenn., 1964*a*.
McGowan, F. K., W. T. Milner, and H. J. Kim, Nuclear cross sections for charged particle induced reactions; Ni, Cu, *Rep. CPX-2,* pp. 132–155, Oak Ridge National Lab., Oak Ridge, Tenn., 1964*b*.
Meadows, J. W., and R. B. Holt, Excitation functions for proton reactions with sodium and magnesium, *Phys. Rev., 83,* 47–49, 1951*a*.
Meadows, J. W., and R. B. Holt, Some excitation functions for protons on magnesium, *Phys. Rev., 83,* 1257, 1951*b*.
Parkin, D. W., and D. Tilles, Influx measurements of extraterrestrial material, *Science, 159,* 936–946, 1968.
Poskanzer, A. M., Range of 1–3 Mev ^{22}Ne ions in Al and the analysis of some ^{24}Na recoil data, *Phys. Rev., 129,* 385–387, 1963.
Price, P. B., and D. O'Sullivan, Lunar cr... rate and solar flare paleontology, *Geochim. ...mochim. Acta,* suppl. 1, vol. 3, 2351–2359, ...
Rancitelli, L. A., R. W. Perkins, W. D. ... and N. A. Wogman, Erosion and mixing of ... lunar surface from cosmogenic and primor... radionuclide measurements in Apollo 12 ... samples, *Geochim. Cosmochim. Acta,* supp... vol. 2, 1757–1772, 1971.
Shedlovsky, J. P., M. Honda, R. C. Reedy, ... Evans, D. Lal, R. M. Lindstrom, A. C. De... J. R. Arnold, H. Loosli, J. S. Fruchter, and ... Finkel, Pattern of bombardment-produced ... dionuclides in rock 10017 and in lunar soil, ...*chim. Cosmochim. Acta,* suppl. 1, vol. 2, ... 1532, 1970.
Tanaka, S., and M. Furukawa, Excitation ... tions for (p, n) reactions with Ti, V, Cr, Fe, ... Ni up to $E_p = 14$ Mev, *J. Phys. Soc. Jap.,* ... 1269–1275, 1959.
Tanaka, S., M. Furukawa, T. Mikumo, S. Iw... M. Yagi, and H. Amano, Reactions of argon ... with alpha-particles, *J. Phys. Soc. Jap.,* ... 952–956, 1960.
Tanaka, S., K. Sakamoto, J. Takagi, ... M. Tsuchimoto, Aluminum-26 and beryllium... in marine sediment, *Science, 160,* 1348–... 1968.
Tanaka, S., M. Furukawa, and M. Chiba, Nuc... reactions of nickel with protons up to 56 M... *J. Inorg. Nucl. Chem.,* in press, 1972.
Wasson, J. T., Radioactivity in interplane... dust, *Icarus, 2,* 54–87, 1963.
Webber, W. R., Evaluation of solar cosmi... event during solar minimum, *Tech. Rep. ... 8427-4,* Space Science Group, Space Div... Boeing Co., Seattle, Wash., 1966.
Webber, W. R., The spectrum and charge com... sition of the primary cosmic radiation, *H... buch der Physik,* vol. 46/2, edited by K. ... pp. 181–264, Springer, New York, 1967.

(Received September 24, 1971;
revised May 2, 1972.)

A Multiple-Scattering Model of the Diffuse Component of Lunar Radar Echoes

JAMES B. POLLACK[1]

Space Science Division, Ames Research Center, NASA
Moffett Field, California 94035

LAIRD WHITEHILL

Laboratory for Planetary Studies, Center for Radiophysics and Space Research
Cornell University, Ithaca, N.Y. 14850

We propose that the average diffuse component of lunar radar echoes results from the cumulative effect of multiple scattering within the ejecta blanket of fresh young craters. Using a multiple-scattering polarization computer program, we compare our model with a variety of observations of the diffuse component and find a general agreement between the two. We show that multiple scattering makes a significant contribution to the partial depolarization of incident completely polarized radar signals, although single scattering may also be important. Mean indices of refraction of 1.3 and 1.6 are inferred for the ejecta blanket at wavelengths of 3.8 and 23 cm, respectively. These values are consistent with measurements made on an Apollo 11 fine sample and indicate an increasing density with depth below the surface. We hypothesize that the difference between the diffuse reflectivities of mare and highland areas is due chiefly to differences between the microwave absorption properties of rocks and dust in the two regions. If that is so, radar maps, properly prepared to display such differences, can serve as geological maps of the mineral or minerals (perhaps ilmenite) that are the principal microwave absorbers.

It is generally believed that two physical mechanisms are jointly responsible for the backscattering of radar signals from the moon: quasi-specular reflection and diffuse scattering [*Hagfors,* 1967]. The first mechanism refers to backscattering from smooth facets of the surface, whereas the second involves scattering by surface or subsurface irregularities, whose size is comparable to the wavelength of observation (centimeter to meter). Quasi-specular reflection causes little if any depolarization of an initially completely polarized signal and leads to a sharp peaking of the returned signal near the subradar point. In contrast, diffuse scattering partially depolarizes and has only a modest dependence on the angular distance from the subradar point. In this paper we will present a model of the diffuse component, which is compared with a number of observed properties of this component. In the rest of this section we review prior efforts to explain the diffuse component, present our model, and discuss evidence that supports it.

Gold [1966] and *Hagfors* [1967] first suggested that rocks were the physical agents responsible for the diffuse component. This hypothesis seems to be very reasonable, since rocks are the most obvious centimeter- to meter-sized irregularities seen on Surveyor and Apollo photographs. Furthermore, rocks are much more numerous in the vicinity of young craters, which are observed as areas of enhanced diffuse reflection. *Hagfors* [1967] suggested that surface rocks distributed more or less uniformly over the lunar surface were responsible for the diffuse scattering and that their nonspherical shape led to the observed partial depolarization. *Burns* [1970] estimated that surface rocks could not cause enough backscattering and so proposed that most of the scattering resulted from single scattering by rocks buried in the regolith and distributed more or less uniformly over the

[1] Part of this work was done while the author was at the Laboratory for Planetary Studies, Center for Radiophysics and Space Research, Cornell University, Ithaca, N.Y. 14850.

lunar surface. Finally, *Thompson et al.* [1970] used Mie scattering to describe the single-scattering properties of the rocks and showed that models with single scattering by surface rocks or multiple scattering by subsurface rocks were capable of accounting for several observed properties of the diffuse component.

Unlike these earlier models, our model proposes that the average diffuse-scattering properties of the moon are chiefly the result of scattering in the interior and the near exterior of small (~1 km) young craters. We also hypothesize that rocks are the chief scattering agents, the scattering taking place within the ejecta blanket. Because the scattering layer is optically thick and the single-scattering albedo is high, as is shown below, one consequence of our model is that multiple scattering is important and makes a significant contribution to depolarization. We will make a detailed comparison with the observed properties of the average diffuse component by using Mie scattering to describe the single-scattering behavior of the rocks and an 'exact' numerical scheme to compute multiple scattering. The model calculations also have rather direct applicability to explaining the characteristics of many radar anomalies, which in our model are simply craters large enough to be resolved with present radar techniques.

There are several lines of evidence that we feel lend strong credence to our model. We can estimate the relative contributions to the average diffuse reflectivity from rocks lying in and near fresh young craters and rocks lying further away. For this purpose we consider a representative fresh crater and divide it and its surrounding area into a series of annuli with inner and outer radii of 0–1r, 1–2r, $\cdots$, 9–10r, where r is the crater radius. Because the fresh young craters of interest cover about 1% of the lunar surface, this division is equivalent to considering the effects of rocks near and far from fresh young craters. The following results are very insensitive to the exact fraction of the area covered by these craters. The relative contribution to the diffuse reflectivity from a given annulus approximately equals the fraction of the area covered by rocks comparable to and larger than the wavelength of interest times the area of the annulus. Table 1 shows the fraction of the area of an annulus covered by blocks of >2 meters for a 380-meter fresh crater in rough mare [*Moore et al.*, 1969]. Multiplying by the relative area of the annuli (in units of πr^2) gives the relative scattering contribution from rocks (Table 1). We see that the area between 0 and 2r contributes 3 times as much to the backscattering as the area beyond 2r and that the area between 0 and 3r contributes about 8 times as much as the remaining external area; that is, even though the region between 0 and 3r covers only about 10% of the total area, it contributes nearly 90% of the total backscattering from rocks. Very analogous results follow for other craters [*Moore et al.*, 1969]. For some of these other craters, values are also given for rocks of >1 meter. The preceding estimate actually underestimates the relative contribution near the crater, since multiple scattering enhances the reflectivity in regions where a large abundance of rocks can be expected. We conclude that, for a wavelength of 70 cm, fresh young craters and their immediate environments are the principal contributors to the average diffuse component arising from scattering by rocks. Because the diffuse component at shorter wavelengths has characteristics very similar to those at 70 cm (e.g., limb-darkening behavior and degree of depolarization), we infer that a similar situation exists at other wavelengths.

TABLE 1. Relative Contributions to the Diffuse Backscattering by Surface Rocks Lying within Annuli Centered about a Fresh Young Crater with a Radius of 380 Meters

Inner and Outer Annulus Radius	Fraction of Area Covered by Rocks of >2 meters	Relative Area of Annulus	Relative Power
0 to 1r	0.096	1	0.096
1r to 2r	0.048	3	0.144
2r to 3r	0.010	5	0.050
3r to 4r	0.003	7	0.021
4r to 5r	0.0013	9	0.012
5r to 6r	0.0003	11	0.003
6r to 10r	≤0.0003*	64	≤0.019

*Inferred from the rest of the table.

Another indication of the validity of our 'discrete source' model is provided by the 3.8-cm radar maps from *Lincoln Laboratory* [1970]. According to most models of the average diffuse component, craters that are large in comparison with the radar resolution element will be observed as bright spots on the maps of this component, since they have a large population of rocks. However, our model also predicts that young craters, which are small in comparison with the resolution element, will also be seen as bright spots. If the area between the young craters were the principal contributor to the average diffuse component, this would not be the case. The Lincoln Laboratory map does show a large number of diffuse bright spots associated with young craters, which are small in comparison with a resolution element.

Next we will outline our computational method; summarize the relevant information about craters needed in our calculations, and compare our model with a large number of properties, including polarization properties, of the average diffuse component. We will conclude with a discussion of the preceding comparison, the applicability of our results to radar anomalies, and a proposed test of our model.

COMPUTATIONAL METHOD

The Stokes' vector is a four-column vector that describes the intensity and the state of polarization of an arbitrary electromagnetic wave [e.g., *Chandrasekhar*, 1950]. Given an arbitrary set of incident Stokes' vectors, we wish to calculate the set of Stokes' vectors that result after multiple scattering by a layer containing rocks. To accomplish this calculation, we used a Mie-scattering computer program to describe the single-scattering behavior of the rocks and a doubling computer program to obtain the resultant radiation after multiple scattering has taken place. All the computer calculations described in this section were carried out by Whitehill. We first describe the Mie calculations and the doubling computations and then their application to the lunar geometry of interest, and finally we examine and partially justify some of the approximations used. The computational method is given in much greater detail elsewhere [*Whitehill*, 1972; *Hansen*, 1971]. The single-scattering phase function describes the dependence of the radiation field on the angle of scatter after a single-scattering event. This parameter was obtained from a Mie-scattering computer program. The input parameters to our program are the real and imaginary indices of refraction (relative to the surrounding medium), the wavelength, and the size-distribution function. These parameters are specified in the next section.

The quantity obtained by these calculations is the single-scattering albedo, the ratio of the amount of light scattered to that absorbed and scattered by the rocks. Before mating these results to the doubling program, we modified the single-scattering albedo to take account of absorption by the dust between successive scattering events in a manner analogous to that used for the line formation problem in scattering atmospheres [*Hansen*, 1969*a*].

The multiple-scattering calculations were performed by the doubling method originally suggested by *van de Hulst* [1963] and generalized to anisotropic phase functions by *Hansen* [1969*b*]. These prior efforts involve scalar intensity equations. We generalized these equations to matrix equations to include polarization [see also *Hansen*, 1971]. An important parameter in these calculations is the optical depth, which is a measure of the probability of scattering and absorption for a beam of radiation passing through a scattering layer [*Chandrasekhar*, 1950]. Briefly, the doubling formalism consists of combining two layers of optical depth τ', whose scattering and transmission matrices are known, to obtain these same matrices for a layer of optical depth $2\tau'$. The initial optical depth is taken to be so small (2^{-25} in our case) that only single scattering need be considered. The program then performs enough doublings to obtain the optical depth of interest.

The result of the doubling procedure is that the scattering matrix S is determined for a scattering layer of total optical depth τ. This matrix, when it is applied to an incident Stokes vector in an arbitrary direction, yields the reflected Stokes vector in a second arbitrary direction. A number of transformations had to be made in the application of these results to our lunar scattering model. These transformations are described in the appendix. In addition to the inputs from the single-scattering program, we must also specify the optical depth of the ejecta blanket, the real part of the index of refraction of the dust medium, and the relative contributions to the scattered radiation from the interior and the exterior of the crater.

The numerical validity of the Mie-scattering program was tested against results given by *Deirmendjian* [1969], whereas the values of the doubling program were compared with those of the Rayleigh-scattering tables of *Coulson et al.*

[1960] and another doubling program independently written by J. E. Hansen (personal communication, 1970) for an anisotropically scattering phase function.

Several approximations were made in the preceding formalism and its application to radar backscattering by the moon.

1. In equation A1 we implicitly neglect radiation that is multiple-scattered by the scattering layer, is subsequently reflected once or more at the top interface, is further scattered, and eventually escapes to space. We justify this neglect on the basis of the low reflection coefficient of the interface (~5%).

2. No account is taken of surface rocks. In contrast to subsurface rocks, no initial and final transmission through the top dust interface is required for surface rocks to backscatter radiation to space. We justify this assumption a posteriori on the basis of certain observations discussed below.

3. The physical properties of the scattering layer are assumed to be the same over both the inside and the outside of the crater and among craters of the same diameter within a given type of mare or highland region. This approximation is forced on us by the lack of sufficient data, but we feel that allowance for it will not substantially change our conclusions.

4. In using Mie-scattering and simple multiple-scattering theories to describe the scattering properties of ejecta blankets, we have made some implicit assumptions, some of which are not entirely valid. We have assumed that the rocks are spherical, that only the far-field component of the scattered radiation need be considered, that the incident radiation in each scattering event is plane parallel, and that shadowing of one rock by another does not occur. The last three assumptions are entirely valid only when the distance between scattering centers is very large in comparison with the wavelength and the size of an average rock, a condition not satisfied within ejecta blankets. Fortunately, for the special case of interest involving subsurface scattering and incident completely polarized radiation, our calculations should be meaningful. Our results depend most sensitively on the value of the single-scattering albedo, a parameter that is insensitive to the exact geometry of the rocks [*Sagan and Pollack*, 1967]. In a number of cases we obtained similar results with single-scattering phase functions that had the same single-scattering albedo but differed greatly in their angular distribution and degree of polarization. The most deleterious effect of these approximations is a neglect of the depolarization arising from single scattering. We preclude allowing for this effect by assuming that the rocks are spherical. Therefore our calculations may be viewed as an attempt to assess the importance of multiple scattering in causing the observed amount of depolarization.

Properties of Lunar Rocks and Craters

To carry out the calculations outlined in the previous section, we must first specify certain characteristics of lunar rocks and craters. The calculations described below are insensitive to many of the parameter choices within their anticipated uncertainties. In the next section we will point out the important parameters for each case. When we are comparing our model with observations of the average diffuse properties of the moon, such as degree of depolarization, we will use the properties of highland regions, since highland regions cover 67% of the surface facing the earth and have a reflectivity per unit area about twice that of the mare areas. Naturally, when we are making comparisons between highlands and maria, we will also need to know the properties of the mare.

We list our choice of relevant crater properties below.

1. The fresh craters of interest are assumed to be paraboloid in shape, having a depth to diameter ratio of 1:4 and a rim height to diameter ratio of 1:25 [*Moore et al.*, 1969].

2. Half the rim height is attributed to ejecta blanket material. The depth of the ejecta blanket inside and outside the craters is taken to be the same [*Carlson and Roberts*, 1963].

3. On the basis of radar scans across Tycho we infer that the interior of fresh craters is responsible for 50 ± 10% of the total diffuse reflectance (T. W. Thompson, personal communication, 1970).

4. The integral number $N(D)$ of fresh craters of size D and larger is given by [*Moore et al.*, 1969]

$$N(D) = (t_e^*/d_e) \times 10^{-1} D_e^{-2} \qquad D < D_e \tag{1}$$

$$N(D) = (t^*/d) \times 10^{-1} D^{-2} \qquad D > D_e$$

where d is the depth of the crater. The crater will cease to be a strong radar anomaly in our model when subsequent saturation bombardment causes all the rocks to be pulverized within a top layer of thickness t^*. This circumstance will occur when the two-way optical depth of this top layer is of the order of 1. From data given below we estimate that t^* is about 6 times the wavelength of observation.

The bound D_e is the size below which fresh craters have only a low density of rocks comparable to the wavelength of interest in their ejecta blankets. Two factors enter here. First, for blocks to be present, the crater must penetrate the regolith. For mare regions this condition means that the crater must be >10 meters in diameter, whereas for highland regions the value may vary from 10 to >100 meters, depending on the highland region under consideration [*Moore et al.*, 1969]. Highland regions that adjoin mare basins and are coeval with them, such as the Apennine mountains, will have values of D_e close to the lower bound given. Unless it is otherwise specified, we will adopt a value of 50 meters as the mean for the highlands. Second, not all craters that penetrate the regolith produce numerous blocks of the size of interest. From data given by *Moore et al.* [1969] we estimate that craters must have a diameter in excess of approximately 400 meters for numerous blocks 1 meter in size to be present. We assume that this second limit scales as the block size and hence as the wavelength.

Next we list our choices of relevant properties of the rocks and the dusty matrix.

1. The differential number of rocks of radius a per unit volume is given by

$$n(a) = 0.017a^{-3.82} \qquad a < 25 \text{ cm}$$

$$n(a) = 0.76a^{-5} \qquad a > 25 \text{ cm}$$

This result is derived from the observed surface distribution function [*Moore et al.*, 1969] and from an application of *Rosiwal's* [1898] principle [*Shoemaker and Morris*, 1968], which states that the fraction of the area covered by surface rocks will equal the fraction of the volume occupied by rocks in a well-mixed layer of material. This condition should be met for the ejecta blanket.

2. The absorption length of a material is the distance over which an electromagnetic wave must travel in the material before being attenuated to $1/e$ of its initial intensity. To within a factor of 2 the absorption length of the dust is 12.5 times the wavelength. This value is derived from thermal and electrical properties of the moon as a whole, inferred from radio and infrared temperature measurements [*Linsky*, 1966] as well as from direct measurement of Apollo 11 fines [*Gold et al.*, 1970].

3. Measurements on the Apollo 11 dust sample for a wide range of compaction conditions yield refractive indices of 1.3–1.6 [*Gold et al.*, 1970], maximum compression yielding the second value.

4. We adopt values of 5 times the wavelength and 2.6 for the absorption length of the rocks and their index of refraction relative to a vacuum, respectively. These values are derived from the measured electrical properties of anorthosite [*Campbell and Ulrichs*, 1969], a proposed major constituent of the highlands [*Wood*, 1970]. On the basis of the variation exhibited by terrestrial rocks [*Campbell and Ulrichs*, 1969], we consider the uncertainties to be factors of 3 and ±0.4, respectively.

We now estimate the optical depth of the scattering layer. Using the above prescriptions for the rock, the volume distribution function, and the thickness of the ejecta blanket, we find that a crater 50 meters in diameter has an optical depth of 1 at a wavelength of 70 cm and that the optical depth varies linearly with crater diameter and inversely with wavelength. At a wavelength of 70 cm we consider only craters whose diameter is >400 meters. Thus the minimum optical depth is about 8. Our calculations below show that the scattering characteristics of a crater having optical depths of >4 are very close to those of a crater having an infinite optical depth. These remarks also hold at other wavelengths. Thus, in some of the calculations in the next section, we use our results for large optical depths. The above estimate also indicates that multiple scattering must be used in the context of our model.

Comparison with Observations

We now apply the formalism of the second section and the parameter choices of the third section to compare our model with the observed properties of the average diffuse component. A typical radar observation consists of sending a

completely polarized signal and observing the two orthogonally polarized components of the returned signal. The observed component that is the same as the one that would be obtained from reflection by a smooth plane is called the polarized component and contains contributions from both quasi-specular and diffuse reflection. Quasi-specular reflection tends to dominate near the subradar point and diffuse reflection near the limb. The other observed component is called the depolarized component and is due solely to diffuse reflection [*Hagfors*, 1967].

To test completely a given model of diffuse scattering, one should verify separately each component of the transformation matrix that converts the incident Stokes vector into the reflected Stokes vector. Although the transformation matrix has 16 components in general, our calculations show that for backscattering (i.e., when the receiver is also the transmitter) there are only five independent matrix elements. A similar result has been obtained by *Hagfors* [1967] from symmetry considerations. As Hagfors showed, it is possible to measure five independent linear combinations of the five matrix elements through judicious choices of the transmitted and received Stokes vectors. We make such a complete comparison below. Each type of measurement is a function of angular position on the moon and of wavelength. The comparisons below are made accordingly.

We first consider the ratio of circularly polarized radiation to depolarized radiation that results from transmitting circularly polarized radiation. Figure 1 shows the theoretical variation of this ratio for various optical depths τ as a function of μ, the cosine of the angular distance from the subradar point. The results have been averaged over annuli of constant μ. The ordinate is the ratio expressed in units of decibel, the conventional unit in radar observations. In Figure 1 the number of decibels equals $\log_{10} P_p/P_D$, where P_p and P_D are the power in the polarized and depolarized components, respectively. We see that the results for optical depths of ≥ 4 are quite close to values obtained for an infinite optical depth. As was explained in the previous section, we will make comparisons in general with models having large optical depths.

The ratio of polarized radiation to depolarized

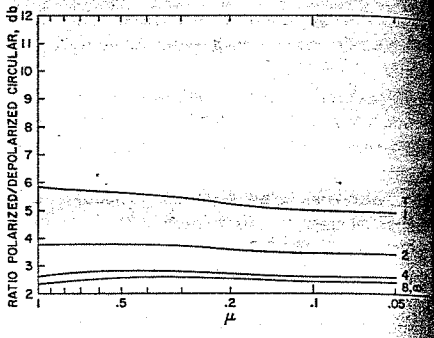

Fig. 1. Ratio of the power in the polarized component to that in the depolarized component as a function of μ, cosine of the angular distance from the subradar point. Circularly polarized radiation has been transmitted and received from range rings of constant μ. The solid curves display the results of theoretical calculations for various optical depths τ of the ejecta blanket. All calculations were performed for a single-scattering albedo of 0.79, indices of refraction of the dust and the rocks relative to the dust of 1.6, and a 50% contribution to the returned echo from the interior of the craters.

radiation depends most sensitively on the single-scattering albedo. Figure 2 shows this dependence for the polarization conditions used in Figure 1. The rise in the observed ratio for values near 1 is due at least in part to a significant contribution to the polarized component from quasi-specular reflection. To a first approximation at small values of μ, both the observed points and our theoretical curves exhibit no strong dependence on μ, owing to the small range of subsurface scattering angles and the averaging over the interior of the crater.

For multiple scattering to be solely responsible for the observed amount of depolarization near the limb, a single-scattering albedo of about 0.9 is required (Figure 2). The curves of this and other figures were calculated with indices of refraction of 1.6 for the dust relative to a vacuum and 1.6 for the rocks relative to the dust. The theoretical curves depend on both variables to some extent. The value for the dust has been chosen to be consistent with the value implied by observations discussed below. If we allow for variations in the second index of refraction of the amounts indicated in the last section, the required single-scattering albedo is 0.9 ± 0.05. Figure 3 shows an analogous

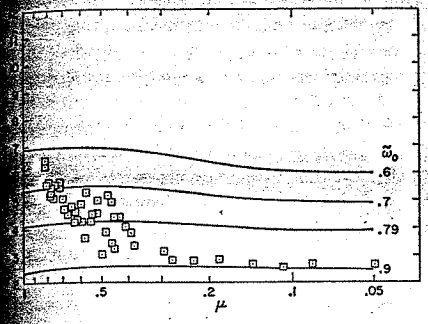

Fig. 2. Ratio of polarized radiation to depolarized radiation as a function of μ. The theoretical results shown in the solid curves were obtained with the polarization conditions and parameters used in Figure 1, except that the optical depth has been taken to be infinite and the single-scattering albedo $\tilde{\omega}_0$ varied. Squares indicate observed values of this ratio obtained at a wavelength of 23 cm.

comparison for incident linearly polarized radiation, and we find that a single-scattering albedo of 0.8 ± 0.05 is required if multiple scattering is the sole source of depolarization. The discrepancy between the estimates for linear and circular polarization will be commented on below.

From the range of parameters (especially the absorption length) given in the last section, it is estimated that for wavelengths shorter than 70 cm the single-scattering albedo expected for the model is $0.8^{+0.1}_{-0.3}$. Thus multiple scattering could conceivably account for all the observed depolarization. Even with the lowest estimated value for the single-scattering albedo, multiple scattering can account for 40% of the observed amount of depolarization. We conclude that multiple scattering is an important source of depolarization.

As a final comparison of our model with the present set of data we consider the wavelength dependence of the ratio of polarized radiation to depolarized radiation. The observed ratio is approximately the same for circular radiation at 3.8- and 23-cm wavelengths and approximately 0.75 db larger at a 70-cm wavelength. The observed difference between the 70-cm value and the value at shorter wavelengths could be produced by lowering the single-scattering albedo by only 0.05 at 70 cm. Using the particle size distribution function given in the last section, we find that the single-scattering albedo is essentially constant between 3.8- and 70-cm wavelengths in agreement with the preceding observations. Unfortunately, we do not know variables such as the particle size distribution function well enough to be able to predict the small change exhibited at a 70-cm wavelength.

We next examine observations in which the circularly polarized radiation is transmitted and the two backscattered linear components are received. Unlike the measurements discussed above, these results refer to radiation scattered from a small part of the surface and are not annuli averages. The linear components analyzed lie within and perpendicular to the meridian plane of incidence. The observed data points for a wavelength of 23 cm are shown by the triangles in Figure 4 along with the theoretical curves for a variety of indices of refraction of the dust. If there were no difference in the received powers of the two linear modes, the data points would lie along a horizontal line at the 10-db level. One explanation for the observed systematic deviations from this value is that single scattering by elongated rocks on the surface is responsible for the return. The sign of the observed deviation requires the long axis of the rocks to be preferentially aligned with the local vertical [*Hagfors*, 1967]. Such a mechanically unstable situation seems unlikely. Alternatively, the scattering may arise at least in part

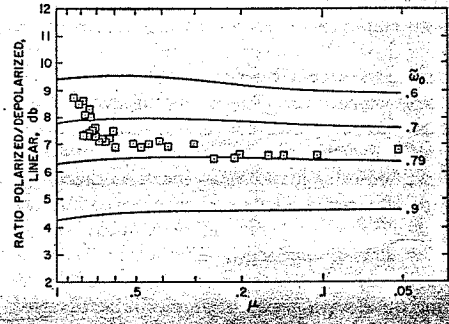

Fig. 3. Ratio of polarized radiation to depolarized radiation as a function of μ. The theoretical results shown by the solid curves were obtained with the parameters used in Figure 2, except that the incident and returned signals are linearly polarized. Squares indicate observations obtained at a wavelength of 23 cm.

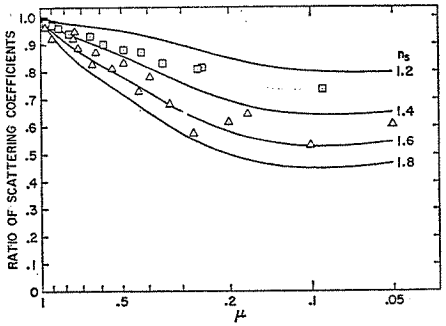

Fig. 4. Ratio of the power in the linearly polarized component lying perpendicular to the incident meridian plane to that lying within this plane as a function of μ. Circularly polarized radiation has been transmitted. The theoretical results were obtained with the parameters used in Figure 1, except that an infinite optical depth was assumed and the index of refraction of the dust varied. Squares and triangles refer to observations at wavelengths of 3.8 and 23 cm, respectively.

from beneath the surface [*Hagfors*, 1967]. The preferential scattering of radiation whose E vector lies in the plane of incidence can be attributed to the preferential transmission of this component into and out of the surface, according to Fresnel's law. The lack of a strong upward turn in the curve at the smallest value of μ provides some justification for the neglect of scattering at the surface in our model. If this scattering were important, it would manifest itself most clearly at the smallest values of μ, for which the slant path optical depth through the surface rocks is greatest.

A comparison between the observed values and the theoretical curves in Figure 4 implies that the effective index of refraction of the dust at 23 cm is about 1.6. Also shown in this figure are data points obtained at a wavelength of 3.8 cm. We infer an index of refraction of 1.3 at this shorter wavelength. The inferred decrease of the refractive index of the dust with decreasing wavelength is expected and will be discussed in the next section. The theoretical curves depend only slightly on the value of the index of refraction of the rocks and on the single-scattering albedo. The theoretical curves, however, depend strongly on the fraction of power returned from the interior of the crater as compared with the amount returned from the exterior. For the uncertainties in the value of this last parameter, which is specified in the preceding section, we estimate an uncertainty of about ± 0.15 for the value inferred at 23 cm and about ± 0.1 for the value at 3.8 cm.

A check on the above interpretation is provided by comparing measurements of the ratio of polarized radiation to depolarized radiation for linear radiation transmitted and received from a small area of the surface with similar measurements averaged over annuli of constant μ. The triangles in Figure 5 correspond to annuli average results and have been discussed earlier, whereas the squares denote measurements for the electric vector of the incident radiation aligned perpendicular to the plane of incidence. Comparing these results for the smaller values of μ, at which diffuse scattering is dominant, we see that the results for the annulus average tend to have more depolarization. Such a result would be expected if the scatterers lie beneath the surface, and hence transmission through the surface influences the observed backscattering. Also shown in the figure is a dotted curve, which is a theoretical curve matching the annulus average data. The solid

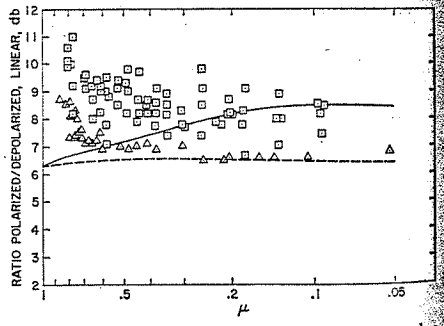

Fig. 5. Ratio of polarized radiation to depolarized radiation for linearly polarized received and transmitted radiation as a function of μ. Theoretical results shown by the dashed curve refer to radiation averaged over a range ring of constant μ, whereas the solid curve indicates corresponding theoretical values for a small element of area, the incident radiation being polarized perpendicular to the incident meridian plane. For both curves the parameters for Figure 4 were used. Triangles and squares refer to observations obtained at a wavelength of 23 cm for a range ring and an element of area, respectively.

curve is a corresponding theoretical curve for the measurements referred to the plane of incidence and has the same parameter choices as the first curve. We see that the two theoretical curves differ at the smaller values of μ by about the same amount that is observed.

The open squares in Figure 6 show the limb-darkening behavior at a 23-cm wavelength for circular polarization transmitted and received in the depolarized mode. We consider only the depolarized mode, since quasi-specular reflection as well as diffuse scattering contributes to the polarized mode. The quantity plotted is power per unit area and is an average over a range ring of constant μ. The observed points vary approximately linearly with μ; that is, to first order the moon is uniformly bright in the depolarized mode. The solid line is the predicted limb-darkening behavior given by our model and is quite insensitive to variations in the choice of parameters within the range specified above. We have adjusted the 0 point of the theoretical curve to match the observed points at $\mu = 0.7$. The tendency of the observed points to fluctuate about the theoretical curve may be due in part to variations in the percentage of highland and mare areas sampled in a given range ring. Highland and mare areas differ significantly in their diffuse reflectivities. The large fluctuations in the observed points near $\mu = 1$ may derive from the same effect, since the amount of area sampled in a given range ring grows small near $\mu = 1$. The descreasing range ring area samples a proportionately smaller number of craters on the average and thus an increase in the statistical fluctuation in power results. Similar statements apply to the depolarization data in Figure 5, where the average over a range ring shows less fluctuation than that over a small area element. Our theoretical calculations assume a smooth moon and thus are not directly valid for μ values smaller than about $\mu = 0.1$, where slope effects can be important. We conclude that our theoretical curve matches the observations quite well and, as we will discuss more fully below, provides a good check on the geometrical features of our model, such as the contribution to the scattering from the interior of the craters. Observations of depolarized circular radiation at 3.8 and 70 cm [*Lincoln Laboratory*, 1970; *Pettingill and Thompson*, 1968] also show a very similar

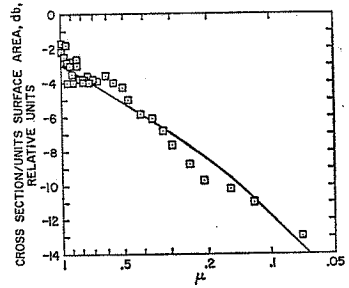

Fig. 6. Cross section per unit surface area in the depolarized mode as a function of μ. The theoretical curve shown by the solid line was obtained for the polarization conditions and parameters used in Figure 2, except that a single-scattering albedo of 0.79 was assumed. Squares indicate observations obtained at a wavelength of 23 cm.

limb-darkening behavior. This insensitivity to wavelength is in accord with the predictions of our model.

We next compare our model with total cross-section data. The observed total diffuse cross section of the moon at 70 cm has been estimated as $1.1 \pm 0.5 \times 10^{-2}\pi R^2$, where R is the radius of the moon [*Pettingill and Thompson*, 1968; *Moore et al.*, 1969]. Using (A3), we predict that the cross section equals approximately $0.8 \times 10^{-2}\pi R^2$. This calculation was done by assuming a single-scattering albedo of 0.8, a relative index of refraction of 1.6 between the rock and dust, and a value of 12.5 times the wavelength for the absorption length. The effect of the uncertainties in the values of these parameters is to produce an uncertainty of nearly an order of magnitude in the computed cross section. We conclude that within very broad limits of uncertainty our model is consistent with the observed absolute value of the diffuse cross section.

The observed diffuse cross section is larger at 3.8 than at 70 cm by about a factor of 2, with the uncertainty being about 50% because of the large uncertainties in the absolute values of the cross sections [*Pettingill and Thompson*, 1968; *Thompson et al.*, 1970]. In estimating the uncertainty in the wavelength dependence of the diffuse cross section we have used the measurement of the polarized diffuse cross section not only at these wavelengths but also at other

wavelengths to better define limits on the wavelength dependence of the polarized cross section. Three parameters contribute to the wavelength dependence: the single-scattering albedo, the index of refraction of the rocks relative to the dust (but not the refractive index of the dust), and the fractional area covered by fresh craters. We estimated above that the single-scattering albedo may have a value that is 0.05 smaller than its value at shorter wavelengths. As a result, the cross section at shorter wavelengths will be 1.3 times that at 70 cm. The index of refraction of the rocks relative to the dust should increase as the wavelength decreases because of the opposite behavior of the index of refraction of the dust relative to a vacuum. This wavelength variation of the refractive index can cause an increase in the cross section toward shorter wavelengths by as much as a factor of 2. The effect of the final parameter, the fractional area covered by fresh craters, is much more difficult to evaluate because it depends sensitively on the depth of the regolith and the variable D_e defined for (1). Neither of these variables is known very well for highland areas. With our nominal values for these quantities the change in the fractional area covered by fresh craters will lead to a decrease in the cross section toward shorter wavelengths by a factor of 2, the uncertainty being a factor of 2 or more. The combined effect of all three parameters is to lead to a poorly defined wavelength variation crudely consistent with the observations.

The depolarized return from mare areas is consistently lower than that from neighboring highlands. Differences ranging from a factor of 2 to a factor of 5 have been found at a wavelength of 70 cm [*Thompson*, 1968], and similar results have been obtained from a preliminary analysis of the data at 3.8 cm (S. Zisk, personal communication, 1970). Within the context of our model we propose that the most important factor affecting the highland-mare differences is the single-scattering albedo, which in turn is determined by the value of the absorption length in rocks and dust. Figure 7 shows the variation of the depolarized cross section as a function of the single-scattering albedo $\tilde{\omega}_0$. We see that changing $\tilde{\omega}_0$ from 0.65 to 0.9 results in a change in the depolarized cross section of a factor of 5, a value near the maximum differences observed between maria and highlands. To first order, $1 - \tilde{\omega}_0$ varies inversely as the absorption length, and hence a change in the absorption length of a factor of only 3.5 would be required to produce a change of a factor of 5 in the depolarized return. Such a variation between highlands and maria seems possible.

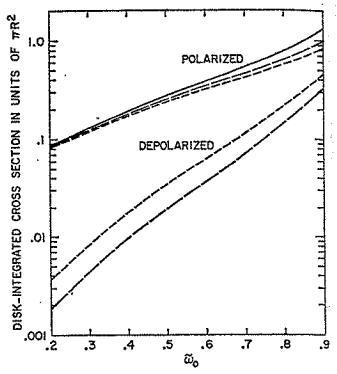

Fig. 7. Disk-integrated cross section in units of πR^2 as a function of the single-scattering albedo $\tilde{\omega}_0$, where R is the radius of the moon. Small-dashed, large-dashed, and solid curves refer to linearly polarized modes, circularly polarized modes, and total returned power, respectively. The theoretical results were obtained for the parameters used in Figure 2, except that the refractive index of the dust was set equal to 1.4 and the scattering took place only in the exterior of the crater. The results displayed are insensitive to these last two parameter choices.

If this suggestion is correct, the depolarized maps can serve as geological maps. We are thus led to ask what mineral or minerals are the dominant absorbers of centimeter wavelength radiation and hence which minerals can be mapped by this technique. At present we can offer no definitive answer. However, measurements by *Chung et al.* [1970] and *Katsube and Collett* [1971] suggest the interesting possibility that ilmenite may be the dominant contributor. The Surveyor α scattering experiment indicated significantly less titanium and, by inference, less ilmenite at the Surveyor 7 highland site than in the mare areas sampled. Such a result is consistent with the highlands' giving larger depolarized returns than the maria. The suggestion that variations in the diffuse reflectivity between individual maria and between mare and highland are due in part to variations in the absorption length can be confirmed by comparing the electrical properties of rocks from the various Apollo sites. In particular we suggest that the absorption length, and hence the single-scattering albedo, is significantly larger for highland rocks. Should this suggestion prove correct, a careful comparison of the electrical properties of individual rocks with their mineralogical properties is needed to establish the principal minerals contributing to the absorption.

DISCUSSION

We first summarize and analyze the results of the preceding comparisons between our discrete source model and the observed properties of the average diffuse component, then discuss the application of the model for understanding large-sized radar anomalies, and conclude with a proposed test of our model.

In the introduction we presented two types of observations indicating that the average diffuse component was due in large measure to the cumulative effect of scattering in the ejecta blanket of fresh young craters. A basic assumption made there was that rocks were the scattering agents. The properties of young craters discussed in the third section implied that the scattering layer of these craters is optically thick, and hence multiple scattering is important. In the last section we made numerical comparisons between our model and a number of observed properties of the diffuse component. In general, the two sets of data were in agreement, although in a number of cases only a crude comparison was possible. Because of a lack of data we were unable to test the model against the observed differences in the diffuse reflectivity of mare and highland regions, but we suggested that the differences were due in large part to variations in the absorption length, reflecting differences in chemical composition, perhaps in the abundance of ilmenite. Examination of Apollo rock samples should test these ideas. Only a crude comparison for the absolute value and the wavelength dependence of the cross section was possible, but within very broad limits the comparison was successful. We discuss the other comparisons in greater detail below.

As is shown in Figure 6, the limb-darkening law predicted by our model is in good agreement with the behavior of the depolarized mode for circular polarization. A μ variation is displayed to first order. In contrast, the limb-darkening produced by the single-scattering effect of surface rocks has no μ dependence [*Thompson et al.*, 1970], and the result of single scattering by subsurface rocks is a $\mu^{3/2}$ law [*Burns*, 1970]. In single scattering by subsurface rocks, the limb darkening results strictly from double transmission through the surface. In sample calculations involving only the exterior ejecta blanket, our multiple-scattering model leads to a dependence of approximately $\mu^{2/3}$. As a result of multiple scattering, the limb darkening resulting from transmission through the surface is smoothed over. Furthermore, because of critical refraction, only a modest range of μ values inside the surface (about 0.8–1) contributes to the radiation emitted to space. Hence, to first order, the multiple scattering does not contribute to the limb darkening other than to partially wash out the initial transmission effect. Because of shadowing, the interior of the crater shows a variation of approximately μ, and so the net effect of the interior and the exterior is a μ dependence slightly less than μ. The preceding discussion indicates that a number of critical aspects of our model determine its limb-darkening behavior: subsurface scattering, multiple scattering, and crater geometry. Thus the agreement displayed in Figure 6 provides support for the model. Similar behavior is predicted and observed at other wavelengths.

Measurements made for small surface areas for incident circular and measured linear polarization implied that most of the scattering arose from beneath the surface. As was discussed above, if backscattering by rocks lying on the surface were contributing significantly to diffuse scattering, it would contribute preferentially at small values of μ and cause an upswing of the points in Figure 4, contrary to the actual observations. The difference observed for the two received modes is believed to arise from transmission through the surface. We inferred values for the index of refraction of the dust of 1.3 ± 0.1 and 1.6 ± 0.15 at wavelengths of 3.8 and 23 cm, respectively. These results pertain to the exterior ejecta blanket, since the interior of the crater causes no differences by virtue of its geometry. These values agree well with the range of values obtained by *Gold et al.* [1970] in their laboratory study of the Apollo 11 dust sample. The corresponding densities are

about 1.0 and 1.6 g/cm³. In comparison, if only the exterior of the crater were considered (flat geometry), the indices of refraction deduced would have been about 1.15 and 1.3. Furthermore, as was pointed out in the discussion of the limb-darkening results, the transmission from the inside to the outside influences our calculations to a greater extent than transmission from the outside to the inside. If transmission into the surface were permitted to have an equal effect, as might occur in some other theory, even lower indices of refraction would be obtained, and it would be difficult to make them compatible with the laboratory measurements referred to above. We attribute the change of refractive index with wavelength to a variation of density with depth. The 3.8-cm results pertain to a shallower depth.

Our model also explains the difference between the ratio of the two linear components observed from a small surface area and that derived from similar data averaged over annuli of constant μ (Figure 5).

We showed that the range of expected single-scattering albedoes leads to a significant contribution to the observed partial depolarization from multiple scattering. At a minimum, multiple scattering will cause 40% of the observed amount of depolarization. We also showed that the ratio of polarized radiation to depolarized radiation in the diffuse mode will not depend strongly on wavelength between 3.8 and 70 cm and that it will not depend strongly on μ, both results being in agreement with the observations. Qualitatively, our model correctly predicts a greater depolarization for circular polarization than for linear polarization, in accord with the observations. However, quantitatively, we predict less of a difference (~2.5 db) than appears to exist (~4 db). This difference can be attributed to the effects of depolarization by single scattering, a circumstance not allowed for in our calculations.

The preceding conclusion on the importance of single scattering is tentative. The two sets of data were obtained on different days and therefore for different subradar points. We know that there are large differences in the diffuse reflectivities of mare and highland areas, and it is conceivable that the areas sampled near the limb on the two days were different enough to bias the ratios of polarized radiation to depolarized radiation. It would therefore be desirable to make new measurements of the two ratios on the same day.

Our model for the average diffuse-scattering behavior has direct applicability to young craters large enough to be resolved by radar mapping techniques. Such craters will be much brighter than their surroundings, especially in the depolarized mode, because the influence of small fresh craters on their surroundings is greatly diluted by the space between them, which contributes little to the diffuse component. The radar maps show such a pattern. We can make some crude comparisons between the expected characteristics of the craters contributing to the average diffuse scattering and those of a large radar-bright crater. We will consider Tycho, since its enhancement is large enough that quasi-specular reflection can be neglected to first order, especially for E-W swaths across it. The observed ratio of circularly polarized radiation to circularly depolarized radiation for Tycho along such a swath is about 2.5 db at 70 cm [*Pettingill and Thompson*, 1968], which may be compared to observed average ratios near the limb of about 2.75 db at wavelengths of 3.8 and 23 cm and 3.5 db at a wavelength of 70 cm. The two sets of values are similar, as we would predict, and the residual differences can be attributed to deviations from the mean in the properties of Tycho, such as the value of the single-scattering albedo and the size at which the break in the rock size distribution function takes place. Using the observed amount of depolarized enhancement and allowing for a difference in the background near Tycho from the mean background of a factor of 2 [*Thompson*, 1968], we estimate that its interior has an effective cross section of $0.4\pi(D^2/4)$, where D is its diameter. The uncertainty in this value is a factor about 2. Our model crater interiors have corresponding values of about $0.75\pi(D^2/4)$ with an uncertainty of a factor of about 3.

Thompson et al. [1971] have made a comparison of infrared and radar anomalies. Most of the anomalies studied are related to impact craters, the youngest craters showing pronounced anomalies of both types. This conclusion is consistent with our model. With increasing age the rocks in the ejecta blanket will be pulverized by small meteorites falling on the ejecta blanket. Thompson et al. also find that the last type of anomaly to disappear is the radar enhancement at the longer wavelengths. This result is in accord with our model and the discussion given by these investigators. It is now believed that infrared anomalies are due to the presence of a large number of centimeter- and meter-sized rocks on the surface. For a crater to show no infrared anomaly but to display an enhancement at 70-cm wavelength, as a number of craters do, requires that the contributing rocks lie below the surface.

The ratio of polarized radiation to depolarized radiation and the diffuse cross section change only slightly over the wavelength range 3.8–70 cm. If our model is correct, there should be a much larger difference between a wavelength of 70 cm and one of $\geq$7.5 meters. This larger difference results chiefly from the break in the distribution of rocks near 1 meter, which implies a significant decrease in the single-scattering albedo. We predict that the circularly depolarized cross section should be lower at 7.5 meters than at 70 cm by a factor of about 10. The uncertainty in this prediction is a factor of about 3. We further predict that near the limb the ratio of circularly polarized radiation to circularly depolarized radiation should be about 10 db at a wavelength of 7.5 meters, the uncertainty being about 5 db. At longer wavelengths, further strong changes should occur. This test of our model would gage the importance of multiple scattering versus single scattering, since any large change in the depolarization ratio can be explained in a single-scattering model only by postulating systematic changes in rock shape with wavelength, an unlikely possibility. We strongly urge that the above annulus average measurements be performed.

We also would like to see some data taken with much better resolutions (<1 km) so that the depolarization ratio could be measured in regions with no visible block fields or fresh craters. We predict that these regions would show little depolarization, the amount being an upper bound on the single-scattering depolarization.

The importance of these suggested measurements is to establish whether depolarized maps can be used to map the moon geologically.

Note added in proof. Analyses of material from the Apollo 11, 12, and 14 sites support our suggestion that the differences in diffuse reflectivity between highland and mare areas result chiefly from a difference in the absorption properties of their rocks and dust. The Apollo 11 and 12 sites were in mare areas. The term highland as used by radar observers refers to regions that date back to the earliest epochs on the moon as well as to the rings of mountainous material surrounding circular maria, which were formed from ejecta of the impact event that created the mare basins. The Apollo 14 sample is a highland area in this latter sense, and, furthermore, its soil composition is quite similar to the soil samples returned by Luna 20 from a highland area of the first type. Our model requires that mare material be 1¾ to 3½ times more absorbing than highland material. *Gold et al.* [1972] find that the Apollo 11 and 12 soil samples are about 3½ and 2 times as absorbing as the Apollo 14 sample. Further, according to the chemical analyses summarized by *Gillum and Ehmann* [1972], there is an approximate linear relationship between the ilmenite content of the soil samples and the absorption coefficients given by *Gold et al.* [1972]. No such correlation is obvious between the other major mineral components and the absorption coefficients. Although the preceding comparisons are very encouraging, further comparisons with material from the remaining Apollo sites are needed before definitive conclusions can be drawn.

APPENDIX

Geometrical transformations. We briefly outline the geometrical transformation used in applying the multiple-scattering results to lunar radar observations. The initial multiple-scattering calculations yield a scattering matrix S, which when applied to the incident Stokes vector yields the reflected Stokes vector. As we will be concerned with scattering within an ejecta blanket and hence with a collection of rocks embedded in a dust medium, allowance has to be made for transmission into and out of the dust medium. This result is accomplished by matrix multiplication by matrices T^e and T^i, where these matrices refer to light leaving and entering the scattering layer. These matrices are defined by *Whitehill* [1972] on the basis of the Fresnel laws. The resultant scattering matrix P is related to S by

$$P = T^e S T^i \qquad (1)$$

Each element of the matrices is a function of the incident and emergent angles. To simplify the calculations up to this point, the matrices have been defined in a rectangular coordinate system whose coordinates lie parallel and perpendicular to the incident meridian plane (i.e., the plane defined by the local normal and the direction of propagation). To relate our calculated matrix P to a set of directions specified by the radar receiver on the earth, we first operate on the incident Stokes vector by a rotation matrix $L(\alpha)$ to transform it into the moon coordinate system and then rotate the resultant P matrix back to the earth coordinate system by multiplying by matrix $L(-\alpha)$. The angle α here is the angle between the two coordinate systems. The result is now a matrix R to be applied to the incident Stokes vector

$$R = L(-\alpha)PL(\alpha) \qquad (2)$$

where matrix multiplication is understood. The matrix $L(\alpha)$ is defined by *Chandrasekhar* [1950].

In many of the applications below, an integration over α must be performed because of variations of the plane of incidence over the portion of the lunar surface of interest. Two types of such integrations occurred: integration over the interior of the crater and integration around an annulus of constant delay. Two further integrations are sometimes required. To calculate the total cross section, we integrate over μ, the cosine of the angular distance from the subradar point. Integration is also required over the crater differential size distribution function $n(D)$ to calculate the absolute diffuse scattering matrix M for the moon, sometimes called the Mueller matrix:

$$M = \int_0^\infty \left[A_{in} + \frac{(1-F)}{F} A_{out} \right] \cdot n(D) \frac{\pi D^2}{4} dD \qquad (3)$$

where D is the crater diameter, A_{in} is the matrix relevant to the interior of the crater, A_{out} is the scattering matrix relevant to the crater exterior, and F is the fraction of the area occupied by the interior of the crater to the sum of the interior and exterior areas. The exterior area is defined as that part of the ejecta blanket significantly contributing to the backscattering. Note that A may depend on D because of the dependence of the optical depth τ and the single-scattering albedo on the size of the crater.

Acknowledgments. We are very grateful to Dr. T. Thompson, Dr. S. Zisk, Dr. J. Hansen, Mr. D. Gault, Dr. W. Quaide, Mr. V. Oberbeck, Mr. R. Reynolds, and Mr. H. Moore for useful discussions.

This work was done partly at Cornell University and supported there in part by NASA grant NGR 33-010-082.

REFERENCES

Burns, A. A., On the wavelength dependence of radar echoes from the moon, *J. Geophys. Res., 75,* 1467–1482, 1970.

Campbell, M. J., and J. Ulrichs, The electrical properties of rocks and their significance for lunar radar observations, *J. Geophys. Res., 74,* 5867–5881, 1969.

Carlson, R. H., and W. A. Roberts, Mass distribution and throwout studies, *Rep. PNE-217,* Boeing Co., Seattle, Wash., 1963.

Chandrasekhar, S., *Radiative Transfer,* pp. 24–35, Oxford University Press, New York, 1950.

Chung, D. H., W. B. Westphal, and G. Simmons, Dielectric properties of Apollo 11 lunar samples and their comparison with earth materials, *J. Geophys. Res., 75,* 6524–6531, 1970.

Coulson, K. L., J. V. Dave, and Z. Sekera, *Tables Related to Radiation Emerging from a Planetary Atmosphere with Rayleigh Scattering,* University of California Press, Berkeley, 1960.

Deirmendjian, D., *Electromagnetic Scattering on Spherical Polydispersions,* Elsevier, New York, 1969.

Gillum, D. E., and W. D. Ehman, Bulk and rare earth abundances in the Luna 16 soil levels A and D (abstract), in *Lunar Science III,* edited by C. Watkins, pp. 274–276, NASA, Houston, Tex., 1972.

Gold, T., The moon's surface, in *The Nature of the Lunar Surface,* edited by D. H. Menzel and J. A. O'Keefe, p. 107, Johns Hopkins Press, Baltimore, Md., 1966.

Gold, T., M. J. Campbell, and B. T. O'Leary, Optical and electrical properties of the lunar surface, *Science, 167,* 707–708, 1970.

Gold, T., E. Belsen, and M. Yerburg, Grain size analyses, optical reflectivity measurements, and determination of high frequency electrical properties for Apollo 14 lunar samples (abstract), in *Lunar Science III,* edited by C. Watkins, pp. 283–285, NASA, Houston, Tex., 1972.

Hagfors, T., A study of the depolarization of lunar radar echoes, *Radio Sci., 2,* 445–465, 1967.

Hansen, J. E., Absorption-line formation in a scattering planetary atmosphere, *Astrophys. J., 158,* 337–349, 1969*a*.

Hansen, J. E., Radiative transfer by doubling very thin layers, *Astrophys. J., 155,* 565–573, 1969*b*.

Hansen, J. E., Multiple scattering of polarized light in planetary atmospheres, 1, The doubling method, *J. Atmos. Sci., 28,* 120–125, 1971.

Katsube, P. J., and L. S. Collett, Electrical properties of Apollo 11 and 12 lunar samples, *Geochim. Cosmochim. Acta,* suppl. 2, 2367–2379, 1971.

Lincoln Laboratory, Radar studies of the moon, final report, Mass. Inst. of Technol., Cambridge, Mass., 1970.

Linsky, J. L., Models of the lunar surface including temperature-dependent thermal properties, *Icarus, 5,* 606–634, 1966.

Moore, H. J., R. J. Pike, and G. E. Ulrich, Lunar terrain and traverse data for lunar roving vehicle design study, open file report, U.S. Geol. Surv., Washington, D.C., 1969.

Pettingill, G. H., and T. W. Thompson, A radar study of the lunar crater Tycho at 3.8-cm and 70-cm wavelengths, *Icarus, 8,* 457–471, 1968.

Rosiwal, A., Uber geometrische Gestemsanalysen, *Verh. Kaiserl. Konigliche, Geol. Reichsanst.,* 143–175, 1898.

Sagan, C., and J. B. Pollack, Anisotropic nonconservative scattering and the clouds of Venus, *J. Geophys. Res., 72,* 469–477, 1967.

Shoemaker, E. M., and E. C. Morris, Size distribution of fragmental debris, Surveyor Project Final Report, Part 2, Science Results, *Tech. Rep. 32-1265,* pp. 86–102, Jet Propul. Lab., Pasadena, Calif., 1968.

Thompson, T. W., Radar studies of the lunar surface emphasizing factors related to selection of landing sites, *Rep. RS-73,* 117 pp., Center for Radiophys. and Space Res., Cornell Univ., Ithaca, N.Y., 1968.

Thompson, T. W., J. B. Pollack, M. J. Campbell, and B. T. O'Leary, Radar maps of the moon at 70-cm wavelength and their interpretation, *Radio Sci., 5,* 253–262, 1970.

Thompson, T. W., H. Masursky, R. W. Shorthill, S. H. Zisk, and G. L. Tyler, A comparison of infrared, radar, and geologic mapping of lunar craters, paper presented at Symposium on the Geophysical Interpretation of the Moon, Lunar Sci. Inst., Houston, Tex., June 1971.

van de Hulst, H. C., A new look at multiple scattering, scientific report, Inst. for Space Stud., New York, 1963.

Whitehill, L., Astronomical applications of Mie theory, Ph.D. thesis, Cornell Univ., Ithaca, N.Y., 1972.

Wood, J. A., Petrology of the lunar soil and geophysical implication, *J. Geophys. Res., 75,* 6497–6513, 1970.

(Received September 7, 1971;
revised April 11, 1972.)